

# Measurement uncertainty analysis in incoherent Doppler lidars by a new scattering approach

Aniceto Belmonte

Department of Signal Theory and Communications, Technical University of Catalonia, 08034 Barcelona, Spain  
[belmonte@tsc.upc.edu](mailto:belmonte@tsc.upc.edu)

Antonio Lázaro

Department of Electronics, Electrics and Automatic Engineering, Rovira Virgili University, 43007 Tarragona, Spain  
[antonioramon.lazaro@urv.net](mailto:antonioramon.lazaro@urv.net)

**Abstract:** We need to examine the uncertainty added to the Doppler measurement process of atmospheric wind speeds of a practical incoherent detection lidar. For this application, the multibeam Fizeau wedge has the advantage over the Fabry-Perot interferometer of defining linear fringe patterns. Unfortunately, the convenience of using the transfer function for angular spectrum transmission has not been available because the non-parallel mirror geometry of Fizeau wedges. In this paper, we extend the spatial-frequency arguments used in Fabry-Perot etalons to the Fizeau geometry by using a generalized scattering matrix method based on the propagation of optical vortices. Our technique opens the door to consider complex, realistic configurations for any Fizeau-based instrument.

© 2006 Optical Society of America

**OCIS codes:** (350.5500) Propagation; (120.3180) Interferometry; (120.6200) Spectrometers and spectroscopic instrumentation; (050.1970) Diffractive optics; (280.3640) Lidar;

---

## References and links

1. M. Born and E. Wolf, *Principles of Optics* (Cambridge University Press, Cambridge, 1999).
  2. M. Endemann, P. Dubock, P. Ingmann, R. Wimmer, D. Morancas, D. Demuth, "The ADM-Aeolus Mission: The first wind-lidar in space," in *Proceedings of 22nd International Laser Radar Conference, ILRC* (ESA SP-561), pp. 953-956.
  3. J. Goodman, *Introduction to Fourier Optics* (McGraw-Hill, Boston, 1996).
  4. G. Hernandez, *Fabry-Perot Interferometers* (Cambridge University Press, Cambridge, 1988).
  5. J. A. McKay, "Assessment of a Multibeam Fizeau Wedge Interferometer for Doppler Wind Lidar," *Appl. Opt.* **41**, 1760-1767 (2002).
  6. A. Lázaro and A. Belmonte, "A unified approach to the analysis of incoherent Doppler lidars: Etalon-based systems," *Opt. Express* (to be published).
  7. J. Brossel, "Multiple-beam localized fringes. Part I. Intensity distribution and localization," *Proc. Phys. Soc. London* **59**, 224-234 (1947).
  8. Y. H. Meyer, "Fringe shape with an interferential wedge," *J. Opt. Soc. Am.* **71**, 1255-1263 (1981).
  9. T. T. Kajava, H. M. Lauranto, and R. R. E. Salomaa, "Fizeau interferometer in spectral measurements," *J. Opt. Soc. Am. B* **10**, 1980-1989 (1993).
  10. T. T. Kajava, H. M. Lauranto, and A. T. Friberg, "Interference pattern of a Fizeau interferometer," *J. Opt. Soc. Am. A* **11**, 2045-2054 (1994).
  11. E. Stoykova, "Transmission of a Gaussian beam by a Fizeau interferential wedge," *J. Opt. Soc. Am. A* **22**, 2756-2765 (2005).
  12. J. R. Rogers, "Fringe shifts in multiple-beam Fizeau interferometry," *J. Opt. Soc. Am.* **72**, 638-643 (1982).
  13. P. H. Langenbeck, "Fizeau interferometer-fringe sharpening," *Appl. Opt.* **9**, 2053-2058 (1970).
  14. J. -M. Gagne, J. -P. Saint-Dizier, and M. Picard, "Methode d'échantillonnage des fonctions deterministes en spectroscopie: application a un spectrometre multicanal par comptage photonique," *Appl. Opt.* **13**, 581-588 (1974).
  15. B. J. Rye and R. M. Hardesty, "Discrete spectral peak estimation in incoherent backscatter heterodyne lidar. I: Spectral accumulation and the Cramer-Rao lower bound," *IEEE Trans. Geosci. Remote Sens.* **31**, 16-27 (1993).
-

## 1. Introduction

Incoherent Doppler lidars for the remote measurement of atmospheric wind profiles base their estimates of frequency shifts on direct detection and high-resolution optical interferometry. In general, Doppler lidars based on Fabry-Perot etalons have been considered as reliable tools to comprehend the atmospheric winds behavior. However, the geometric mismatch of circular fringes to the rectilinear formats of spatially resolving detectors on standard Fabry-Perot interferometers has elicited the development of incoherent multibeam Fizeau wedge interferometers intended to use in incoherent lidars. The Fizeau interference linear fringes, obtained by means of the varying distance between the two plates of the wedge [1], allow the static scanning of spectral features without any additional optics at the interferometer exit and with the high resolving power required by lidar applications.

Measurements of tropospheric wind distributions require estimations to be made simultaneously in the molecular-driven upper troposphere and in the aerosol-laden atmospheric boundary layer close to the ground. Although direct-detection wind lidars can have the capability to resolve both aerosol and molecular backscattering, the spectral widths of these signals are orders of magnitude different, and the interferometer in these instruments must be optimized for either one or the other. Consequently, planned lidar systems use two different interferometers coupled to utilize efficiently all the light coming from aerosol and molecular atmospheric constituents into the detection system [2]. An additional tandem pair of etalons is frequently present as solar background filter.

These multiple interferometer systems, combining both etalon and Fizeau filtering features, pose the considerable challenge of establishing analytical tools for evaluating their design and main spectrometric capabilities. Also, tools are necessary to properly examine the uncertainty added to the Doppler measurement process of atmospheric wind speeds of any practical incoherent detection lidar. The statistic uncertainty of incoherent return fluctuations in lidar systems profiling the atmosphere translate into a lessening of accuracy and sensitivity of any practical Doppler measurement.

For the use of lidar systems based on just Fabry-Perot resonators, partial theoretical treatments have been available on the basis of using instrument transfer functions for angular spectrum transmission [3, 4]. On the other hand, treating instruments including Fizeau wedge interferometers on their design might involve some difficulty and confusion arising from the fact that the existing theoretical formulation adequate for an etalon interferometer cannot be applied as is. No transfer function exists in principle, because the nonparallel mirror geometry would produce a series of transmitted beams whose spatial frequencies gradually drift from the input spatial frequency with increasing number of cavity reflections. Without any transfer function it is necessary to resort to numerical approaches by taking advantage of a direct theoretical description available in the spatial domain. Unfortunately, this approach limits the extent and accuracy of the analytical evaluation of the performance of most practical lidar system considering Fizeau interferometry. Analysis are used to be valid just in the limit regime were Fizeau fringes can be considered equivalent to Airy fringes in a Fabry-Perot with the output mapped in a linear space [5]. In this case, the optimal values for the Fizeau are similar to those for the Fabry-Perot. Conscious of the inherent limitations in the standard techniques used to study this kind of Doppler systems, our research has been focused on tackled this specific problem.

The usefulness of both Fabry-Perot and Fizeau interferometers as spectroscopic instruments is based on narrow fringes whose instrumental shape must be well known. With the aid of Fourier arguments, the spatio-spectral transfer function of an ideal Fabry-Perot etalon allows to describe its transmission features as an optical filtration process acting on both the optical frequency and the spatial frequency of a transmitted beam. We have extent these results further to examine any intensity modulation arising from resonance spatial frequency shift, multiple interferometric coupling, and arbitray nonnormal beam illumination by considering a generalized modal scattering matrix theory as a fast, efficient approach to the analysis of interferometric systems [6]. In contrast with other methods, the new technique is

based on the propagation of Bessel beams, a well-known kind of optical vortices, and allows solving both multilayered reflections problems and spatial diffraction phenomena using scattering parameters associated with the transmitted and reflected vortical spectrum. As in a Fourier plane-wave transformation the angular spectrum is sampled with delta functions, now the spectrum is sampled with circular masses.

In this study we intend to extend the spatial-frequency arguments considered in interferometric systems based on Fabry-Perot etalons to the Fizeau geometry (Section 2) in order to make possible to consider complex, realistic lidar configurations regarding multiple interferometer systems in which Fabry-Perot fringes cannot be considered a good approximation to the spectral output of the instrument. In Section 3, we have chosen to show the sensitivity of the method by studying the wind measurement uncertainty inherent to the lidar instrumentation as an indication of the performance of systems based on etalon and Fizeau interferometers. Of the most practical importance, we consider the interest of using the scattering matrix method to explain the coupling among Fizeau wedges and Fabry-Perot etalons in high-resolution lidar systems.

## 2. Fizeau scattering matrix

New, more advanced lidar instruments are considering Fizeau interferometers for many practical reasons and, consequently, no study on the performance of realistic incoherent lidars is completed without making an allowance for Fizeau-based systems. By using a more general formulation for the scattering parameters, we are allowed to use our formalism in optical devices such as the Fizeau wedges with an inherent angular nonlinear behavior. In order to define the proper Fizeau S-matrix, we are compelled to challenge our technique and consider the convenience of using the transfer function for angular spectrum transmission.

Nonparallelism in the Fizeau wedge (see Fig. 1) produces transmitted beams whose spatial frequency gradually drift from the input spatial frequency with increasing number of cavity reflections. The shift on the angular features avoid considering the convenience of using the transfer function for angular spectrum transmission. Anyhow, it is still possible to resort to numerical approaches addressing the Fizeau angular response by exploiting a direct theoretical description available in the spatial domain [7]. Based on geometrical optics, the method roughly predicts position and asymmetry of the fringes, peak height reduction, and strength of the spurious Fizeau fringes [8-11]. However, any intensity modulation occurring for the coupling of multiple interferometers in complex, realistic lidar systems needs to be inferred by the interference between counter propagating light waves and consider diffraction-induced divergences not described by geometrical optics. In this study, we intend to define a generalized, vortice-based scattering matrix considering all the angular spectrum characteristics needed to describe the performance of multibeam Fizeau wedges.

In the framework of our approach, an optical system can be considered as a set of multiports connected to one another [6]. Here, the scattering parameters describe the interrelationship of the set of incoming  $\mathbf{a}_i$  and outgoing  $\mathbf{b}_i$  normalized waves at the  $i$ th port of the network. Although generally complex systems are multiports, a large number of optical elements (e.g., lens, filters, beam splitters) may be expressed as two-port elements described by the incident, transmitted, and reflected normalized waves. The scattering matrix  $S$  formulation represents the relationships among these normalized wave variables for any optical element as well as an entire system. By definition of scattering parameters,  $S_{ki} = \mathbf{b}_i / \mathbf{a}_k$  equals the wave transformation between the  $k$ th port and the  $i$ th port of a multiport optical system and  $|S_{ik}|^2$  represents the power gain between the  $k$ th and the  $i$ th ports. For the simple two-port elements, the scattering parameters will define a  $2 \times 2$  complex scattering matrix.

Arbitrary optical excitations at the  $i$ th port of the network require a generalization of the scattering matrix formulation. In a general case, with two dimensional spatial signals  $E_i$  going into the optical system, a transform based on Bessel beams is a natural generalization of Fourier techniques:

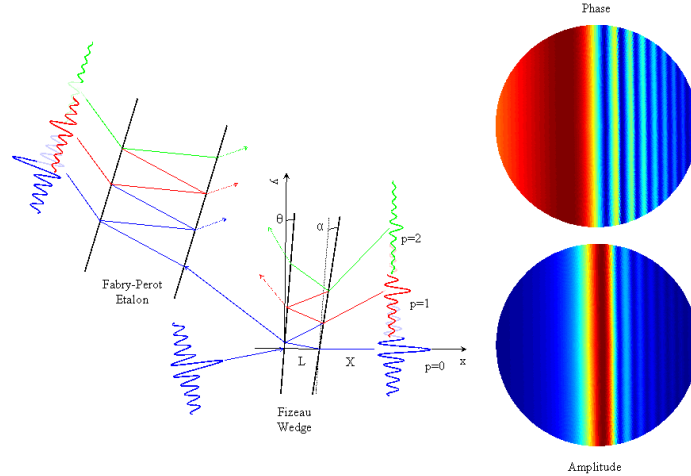


Fig. 1. Optical geometry of a Fizeau interferometer with wedge angle  $\alpha$ , optical thickness  $L$ , and incidence angle  $\theta$ . The interference pattern of the Fizeau detected behind the wedge at distance  $X$  shows unique phase and amplitude features (right). Multiple interferometer systems (left), combining both etalon and Fizeau filters, pose the considerable challenge of establishing analytical tools for evaluating their design and main spectrometric capabilities.

$$E_i(\rho, \phi) = \sum_{m=-M}^M \sum_{n=0}^N a_{nm} J_m(v_n \rho) e^{-jm\phi}, \quad (1)$$

where  $J_m$  is the  $m$ th-order Bessel function of the first kind and  $v_n$  the spatial frequencies of the harmonic functions describing the complex amplitude  $U$ . The angles  $\theta_n$  of the wavevector are related to the spatial frequencies  $v_n$  by  $\sin\theta_n = \lambda v_n$ , where  $\lambda$  is the wavelength of light [3]. The product of these Bessel functions with the harmonic functions in Eq. (1) defines the so-called Bessel beams. A number of  $N_{mn} = (2M+1) \times (N+1)$  modes is considered. Now, we have to consider a set of simultaneous  $N_{mn}$  vortical Bessel beams arriving and leaving at every port considered in our system, and to establish the relationship of everyone with each other [6]. For a two-port optical element we define a  $2N_{mn} \times 2N_{mn}$  complex scattering matrix. We need to consider a scattering matrix for any of the optical elements encountered in our practical optical systems. These matrix elements can be regarded as a library of necessary information and relations used to depict optical systems of any topology.

Although in general is straightforward to define the scattering matrix for simple optical elements, the nonstationarity features of the Fizeau wedge deserve a special remark. As previously stated, outgoing waves from any of its surfaces will show a drift of their angular features that will deter to establish a direct relation with the incoming waves. As depicted in Fig. 1, let's consider a Bessel beam arriving with incidence angle  $\theta$  to a Fizeau characterized by its wedge angle  $\alpha$ . Because of multiple reflections at wedge surfaces, any incoming way is split into a set of waves, the propagation direction of which successively differ by twice the wedge angle  $\alpha$ . The transmitted light  $E_k$  at  $k$ th port consists of a set of  $p=1, 2, \dots, N_p$  Bessel modes  $V_{mn,p}$  emerging with diverging angles  $\theta_p$  and sharing the energy  $|a_{nm}|^2$  of each incident Bessel beam:

$$E_k(\rho, \phi) = \left\{ \sum_{p=1}^{N_p} TR^{(p-1)} e^{j[\theta+2(p-1)\alpha]} \right\} E_i(\rho, \phi), \quad (2)$$

where the incident light  $E_i$  at  $i$ th port is given by Eq. (1). From the laws of reflection and refraction,  $\sin\theta_p = \sin[\theta + 2(p-1)\alpha]$ . As in the classic harmonic analysis, the angle of the wavevector  $\theta_p$  is related to a new corresponding spatial frequency  $\nu_p$  by  $\sin\theta_p = \lambda\nu_p$ . Here,  $\mathcal{R}$  and  $\mathcal{T}$  are the complex reflectivity and transmissivity of the plate surfaces. The bracket term in Eq. (2) is the scattering transmission parameter  $S_{ki}$ . We use a similar expression for the reflected parameter  $S_{ji}$  on the Fizeau surfaces.

In our model, the Fizeau scattering matrix incorporates scattering parameters for both the initial waves in Eq. (1) and the new drifted ones given by Eq. (2). The number of drifted wave terms  $N$  that has to be taken into account depends on the mirror reflectivity  $\mathcal{R}$  [12, 13]. Relevant to the goals of this study, if the Fizeau wedge were to be inserted into a much larger optical system, such as our incoherent lidar systems, all those drifted waves will be considered naturally by the formalism and no further considerations are needed. As expected in real systems, those additional waves will propagate, interfere, and diffract in any other element defining our optical setup.

### 3. Uncertainty in incoherent Doppler measurements

We examine the uncertainty added to the Doppler measurement process of atmospheric wind speeds of any practical incoherent detection lidar, based on either Fabry-Perot etalons or Fizeau wedges, and use our scattering matrix approach to develop efficient working models. The frequency Doppler measurement uncertainty is characterized by its normalized standard deviation  $\delta f$ . Here, we just consider the intrinsic limitation on the determination of the center frequency  $f$  of the signal that is due to the statistical nature of the sampling of the interferometer fringes [14, 15]. We calculate Gagné Doppler measurement uncertainty [14], as a ratio to the Cramer-Rao limit of the measurement of the centroid frequency with a perfect, lossless receiver [15]. Optimal Fizeau parameters are those producing frequency measurement errors close to this ideal Cramer-Rao limit. Gagné's expression for the statistical variance  $(\delta f)^2$  in the determination of the center frequency

$$(\delta f)^2 = \frac{\sum_{-\infty}^{\infty} f_i^2 S(f_i)}{\left[ \sum_{-\infty}^{\infty} S(f_i) \right]^2} \quad (3)$$

considers the signal (photons) going through the interferometer at frequency  $f_i$ , and they are measured with respect to the center frequency of the spectral line. On the other hand, the Cramer-Rao lower bound for the maximum likelihood estimator of the Gaussian central frequency

$$(\delta f)^2 = \frac{\Delta f^2}{2N_0} \quad (4)$$

can be obtained by applying Eq. (3) to a Gaussian distribution with  $1/e$  half-width  $\Delta f$ . The coefficient  $N_0$  is the total signal (photons) transmitted through the interferometric device to be characterized. This assumes that just one spectral range of the interferometer is illuminated.

First, we show the result of applying our techniques to a tandem of two Fabry-Perot resonators acting as an incoherent Doppler interferometric system aimed to measure Doppler shifts. Direct detection Doppler lidars probing atmospheric winds need to consider both Mie scattering from aerosols in the lower troposphere and Rayleigh scattering from the lower stratosphere. As it was indicated before, the spectral widths of aerosol (MHz) and molecular (GHz) backscattered signals are orders of magnitude different (Fig.2, right), and two different interferometric channels must be defined in any reliable working lidar system. Figure 2 (right) shows molecular and aerosol signal components on the molecular and aerosol channels when the light reflected by the aerosol etalon is transmitted by a second molecular etalon. The bites

in the spectrum received on the molecular channel as a consequence of the light transmitted by the aerosol channel are just evident on signals coming from the atmospheric boundary layer, where the aerosol load is more important. In an effort to increase the overall system efficiency, usual instrument configurations capture the light reflected by a high-spectral-resolution aerosol Fabry-Perot etalon into another wider passband molecular etalon. Figure 2 (left) shows a simple schematic of our analysis. In general, interference filters and low-resolution etalons (not show in the figure) block any background radiation for both Mie and Rayleigh channels. A quarter wave plate, modeled as an optical circulator, is used to separate the two spectral channels in our study. Certainly, the analysis and optimization of such complex instruments has to consider in a realistic way the limitations caused by any cross-talk between light channels and any interference and diffractive effect.

Figures 3 and 4 consider the importance of those effects and the capabilities of our technique by showing the analysis of Doppler measurement uncertainty. In the 355-nm working-wavelength system considered in these figures, the aerosol channel analyze aerosol backscattered light with a spectral width of 30 MHz by using a high-resolution etalon with spacing  $d=300$  mm and symmetric mirror reflectivities of  $\mathcal{R}=0.9$ . The molecular-driven light (1-GHz spectral width) reflected in the aerosol channel impinges a second middle-resolution etalon whose mirrors ( $\mathcal{R}=0.74$ ) are spaced a distance  $d=16$  mm. Realistically, and with the intention of blocking any solar background, at the input of this two-channel interferometric instrument a low resolution Fabry-Perot (2-mm spacing, 70% reflectivity) has been also added to the analyzed design. Working etalon apertures are made to match the instrument etendue. If etalon apertures are different, diffraction losses and spreading need to be consider in the uncertainty estimations. Our method takes these effects into account naturally.

In Fig. 3, we show the normalized Doppler measurement errors for both Fabry-Perot interferometers as a function of etalon separation mistuning relative to their nominal spacing  $d$ . Due to the unavoidable illumination coupling between channels (reflected light in the aerosol channel goes into the molecular one), a displacement mistuning on any of the two considered etalons affects the uncertainty on both measurement channels. In fact, a small

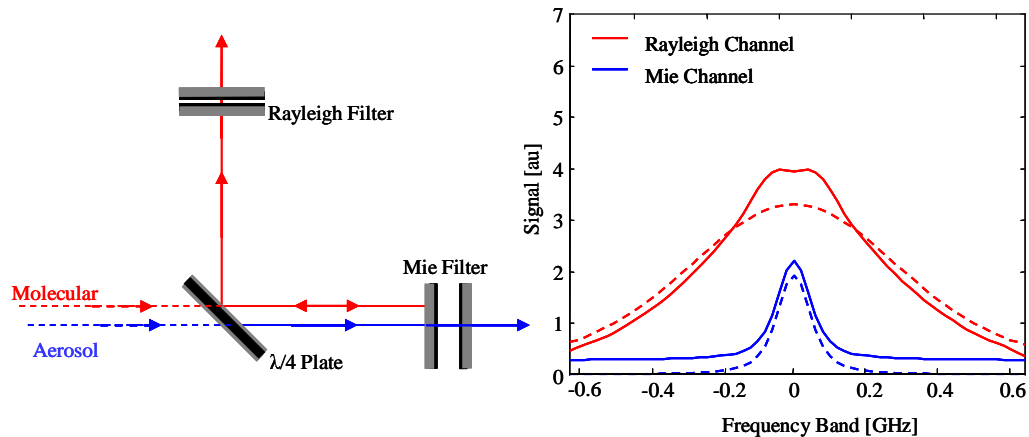


Fig. 2. In our analysis, two high-resolution filters (left) based on interferometric devices are used to separate the Mie (aerosol) and the Rayleigh (molecular) channels. Although the Rayleigh channel is always based on a Fabry-Perot etalon, the Mie channel can be based on either an etalon or a Fizeau interferometer. Although we have considered both cases in this study, the signals transmitted through the interferometers and shown in the figure (right) consider etalon-based systems. The bites in the spectrum received on the molecular channel are just evident on signals coming from the atmospheric boundary layer, where the aerosol load is more important. The atmospheric return signals (dashed lines) are also shown in the figures.

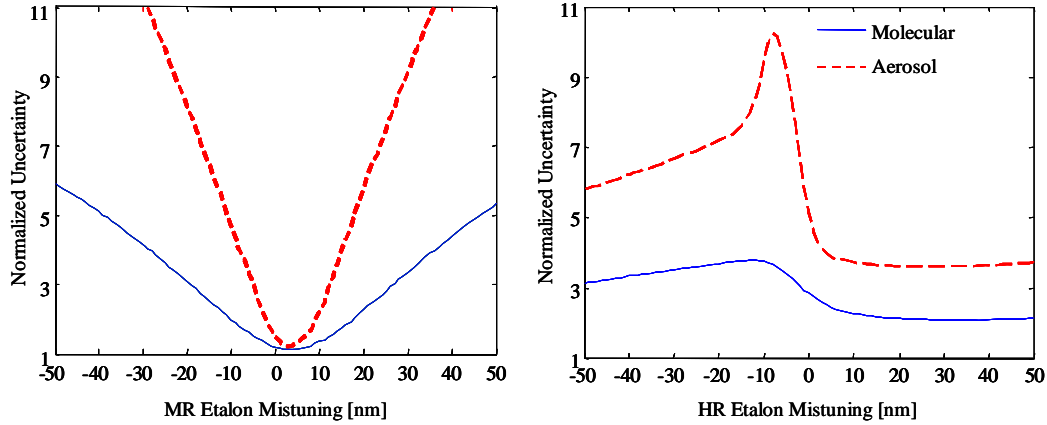


Fig. 3. Normalized Doppler measurement errors for Fabry-Perot interferometric systems as a function of etalon separation mistuning. Middle-resolution (left) and high-resolution (right) etalon systems are considered along with several different etalon reflectivities (finesse).

mistuning of a few nm may translate into a significant increase on the measurement uncertainties. The effect is most relevant for the measurement using aerosol-backscattered light, where a mere 10-nm mistuning in any of the two etalons makes the uncertainty to reach levels with the potential to make the instrument unreliable (normalized uncertainties close to 10). Certainly, it is possible to optimize the separation between the etalon mirrors allowing slight improvements of the system performance. It is also worth to comment the lack of symmetry in our error estimations. More clearly show when the high-resolution etalon mistuning is analyzed (Fig. 3, right), the asymmetry comes from the inherent unevenness of the distance  $\Delta$  between adjacent peaks in the spatial-frequency etalon spectral transmission.

For increasing spatial frequencies (here we sample the spectrum at the frequencies  $\nu_{mn}$  associated with the Bessel waves used in the modal analysis), this spatial free spectral range  $\Delta$

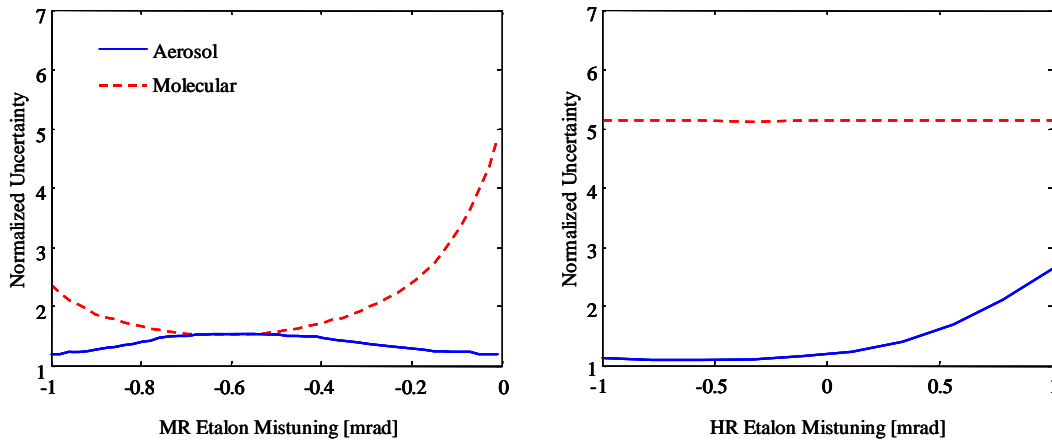


Fig. 4. Normalized Doppler measurement errors for Fabry-Perot interferometric systems as a function of etalon angular misalignments. Middle-resolution (left) and high-resolution (right) etalon systems are considered.

is decreasing. As an increase of the etalon spacing  $d$  moves the etalon spectrum —used to estimate Doppler shift— on the opposite direction that a similar decrease of the spacing magnitude does, the asymmetry of the spectrum translate into an asymmetry of the system sensitivity to the mistuning. Our technique, based on a full electromagnetic estimation considering a realistic propagation of any spatial mode  $v_{mn}$ , is uniquely suited to deal accurately with this kind of critical aspects of etalon behavior scarcely pondered in previous analysis.

Figure 4 repeat the uncertainty analysis for both channels but now we consider the effects of illumination angular mistuning with respect to an initial straight angle of incidence. Once again, angular mistuning in any of the etalon input surfaces translate into modifications of the measurement uncertainties in both channels. Clearly, a mistuning of less than 1 mrad on the middle-resolution etalon may translate into a beneficial decrease of the error on the aerosol channel (Fig. 4, left). Once again, our technique allows to fully comprehending the lop-sidedness of the problem showing the dependency of the normalized error with the sign of the angular mistuning.

Although there have been previous analysis of Fizeau interferometers employing intensive numerical calculations [8-10], the lack of flexibility on these techniques has limited the accuracy of any analysis on the wedge measurement uncertainty. Our technique describes an accurate method of determining the main features of the multibeam fringes and its effects on the error measurement. In Fig. 5, we consider the performance of different Fizeau wedge interferometers. In any of the cases considered in this figure, the wedge angle is set to  $\alpha=25$   $\mu$ rad and the mirror reflectivity to  $\mathcal{R}=0.9$  (resonator etalon finesse  $\mathcal{F}=30$ ). We explore different optical thickness ranging from  $L=15$  mm (frequency spacing of adjacent modes of  $\Delta\nu_{FSR}=10$  GHz and mode FWHM spectral width of  $\Delta\nu=333$  MHz) to  $L=45$  mm ( $\Delta\nu_{FSR}=3.3$  GHz and  $\Delta\nu=111$  MHz). In the analysis, with a working wavelength  $\lambda$  of 355 nm, the Fizeau wedges act as optical filters with resolutions ranging from 0.15 to 0.05 pm. Such filters are suitable for spectral measurements of molecular-backscattered light, with typical linewidth  $\Delta\nu_e$  of a few GHz, or aerosol-backscattered light, where the atmospheric broadening of the laser source spectral linewidth can be neglected and  $\Delta\nu_e$  is in the order of 100 MHz.

In order to increase the usefulness of the Fizeau interferometer as a lidar device with high measurement accuracy, we look for incidence angles resulting in the sharpest interference fringes. We consider realistic situations where the fringes are asymmetric, displaced slightly from the ideal location, and where spurious fringes rest energy from the principal maximum. If the intensity pattern is detected at a fixed distance  $X$  from the wedge and the angle of incidence is changed, a clear interference fringe is observed only within a narrow range of angles. This is illustrated in Fig. 5 (left), which shows that the most favorable conditions for constructive interference for our set of Fizeau wedges occur when the angle of incidence  $|\theta|$  is chosen between 1.0 and 1.2 mrad. For these angles, the fringe sharpness is at its maximum and the transfer of energy from the fringe peak to secondary fringes is minimized. This off-axis illumination compensates part of the optical path differences among the beams emerging from the wedge and whose interference tends to degrade the fringes. Once the ideal incidence angles are set in our analysis, we can further optimize the performance of our Fizeau filters by changing slightly the true effective thickness of the wedges (see Fig. 5, right). Small modifications (less than 10 nm in the examples considered in the figure) of the effective wedge thickness may improve significantly the probable performance of our interferometer by displacing the already sharp interference fringes from its ideal position.

A system which uses the light reflected from a aerosol Fizeau wedge resolving the narrow spectral signature obtained from aerosol backscatter as the input to a molecular etalon intended to observe the molecular backscatter seems to be an efficient way of using the light coming into the lidar receiver. Complementary to the results show in Figs. 3 and 4, where the coupling of several Fabry-Perot etalons were considered, we are also set to address with this study multiple interferometer systems combining both etalon and Fizeau filtering features (Figs. 1 and 2 show the problem schematics). These instrumental configurations are especially relevant to our vortex approach, as any other standard techniques intended to evaluate their

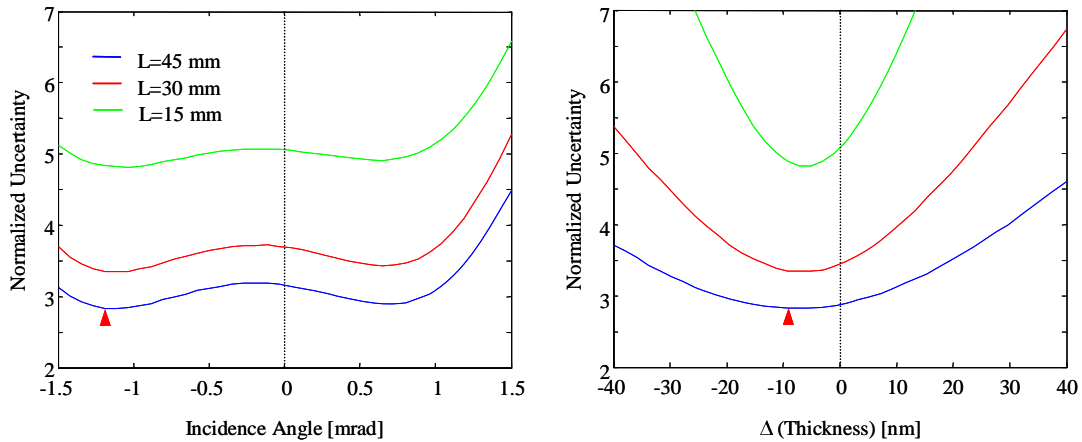


Fig. 5. Doppler measurement uncertainty as a ratio to the Cramer-Rao limit of the measurement of the Gaussian centroid frequency with a perfect, lossless receiver. Modifying the angle of incidence  $\theta$  of the incoming light is possible to achieve most favorable conditions for any of the cases considered in the figure (left). Using the optimal incidence angles (see marker), we further optimize the uncertainty measurement by slightly changing the optical thickness of the Fizeau (right).

design and spectrometric capabilities may find serious difficulties. In particular, in Fig. 6 we consider a system where the light reflected from the Fizeau optical wedge ( $\alpha=12 \mu\text{rad}$ ;  $L=60 \text{ mm}$ ;  $\mathcal{R}=0.92$ ) defining an aerosol channel ( $\Delta\nu_{FSR}=2.5 \text{ GHz}$ ;  $\Delta\nu=66 \text{ MHz}$ ,  $\Delta\nu_e=30 \text{ MHz}$ ) is captured into a Fabry-Perot etalon ( $L=6 \text{ mm}$ ;  $\mathcal{R}=0.75$ ) with a much broader passband ( $\Delta\nu_{FSR}=25 \text{ GHz}$ ;  $\Delta\nu=2.5 \text{ GHz}$ ) to make possible Doppler estimations from molecular-backscattered light ( $\Delta\nu_e=1 \text{ GHz}$ ). Figure 6 shows normalized Doppler measurement uncertainty on both the aerosol and molecular channels as a function of the incidence angle  $\theta$

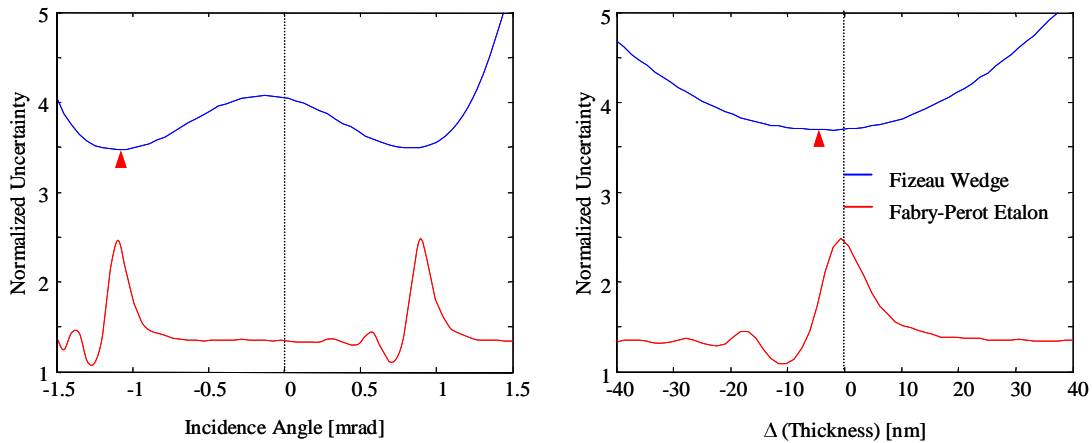


Fig. 6. The analysis of normalized Doppler measurement uncertainty for a multiple interferometer system combining a Fizeau wedge (Mie channel, in blue) and a Fabry-Perot etalon (Rayleigh channel, in red) shows the coupling between both devices. Those incidence angle and optical thickness optimizing the performance of the Fizeau channel (see markers) increase the error measurement on the Fabry-Perot channel.

and optical thickness variations  $\Delta L$  on the Fizeau wedge. As happened in Fig. 5, by chosen pertinent Fizeau wedge parameters, we could optimize the performance of the aerosol channel. Once again, incidence angles slightly larger than 1 mrad (Fig. 3, left) and optical thickness a few nm smaller than the wedge nominal value (Fig. 6, right) translate into improved Doppler measurements. However, the coupling between Mie and Rayleigh channels translate into a suboptimal Fabry-Perot measurement uncertainty. By changing both the incidence angle and thickness of the wedge, we are also modifying the illumination pattern incoming into the molecular etalon in an uncertain way. Although most of the energy arriving into the Fabry-Perot comes from the first direct reflection on the Fizeau surface, a small but significant component of the incoming signal is due to multiple reflections on the wedge mirrors and whose propagation directions differ by twice the wedge angle  $\alpha$ . In most situations, the multibeam Fizeau effects appear on the Fabry-Perot interference fringes. Any realistic analysis of the performance of multiple interferometric incoherent lidar system needs to consider these genuine effects. Optimization of the Fabry-Perot based molecular channel will be strongly affected by the diverging beams coming from the Fizeau wedge.

#### 4. Conclusions

The behavior of an incoherent Doppler lidar can be efficiently analyzed in terms of normalized wave variables at the ports of optical components described by generalized scattering matrices. The new transfer matrix uses Bessel beam as the basic modal expansion characterizing optical signals. The tactic allows solving both multilayered reflections problems and spatial diffraction phenomena using scattering parameters associated with the transmitted and reflected vortical spectrum. In this paper, we extend the spatial-frequency arguments to the Fizeau geometry by using a generalized scattering matrix method based on the propagation of optical vortices. Our technique opens the door to consider complex, realistic configurations for any Fizeau-based instrument.

A glimpse of the inherent statistic uncertainty of incoherent Doppler measurements has been presented paying special attention to the most significant parameters describing the interferometric behavior of Fabry-Perot etalons and Fizeau wedges. Our results, while preliminary, indicate a strong sensitivity of the normalized uncertainty on the tuning of the interferometric devices in their transmission peaks. Optical thickness and incidence angle seem to be notably important in the uncertainty performance of the interferometers. Especially relevant to our vortex technique, it is the possibility of studying in an uncomplicated way complex lidar systems coupling Fabry-Perot and Fizeau interferometers. Unlike in methods considering numerical approaches, for which there is no simple way to comprehend the effects of the Fizeau nonlinearities on etalons, our technique is a feasible tool for computing and analyzing the fields on any optical port and determining the performance of the incoherent lidar. All the results shown in this work have been carried out in the framework of *VBS* (Vortical Beam Spectra), a flexible software tool implementing our generalized scattering matrix theory.

Extension of the method to include in any practical instrument configuration more common optical elements is straightforward, and our analysis has taken into account realistically many other illumination profiles and non-uniform atmospheric conditions. Also, although it is not difficult to consider optical aberrations (by defining scattering matrices associated to phase screens) or optical surface roughness (using a sensitivity analysis) into our estimations, our results are still preliminary in this area. Details are beyond the scope of this paper and we have avoided discussing all these important considerations on the results presented here. We mean to address them in a subsequent study.